Macromolecules

pubs.acs.org/Macromolecules Article

Toughening Biodegradable Isotactic Poly(3-hydroxybutyrate) via Stereoselective Copolymerization of a Diolide and Lactones

Xiaoyan Tang,* Changxia Shi, Zhen Zhang, and Eugene Y.-X. Chen*

Cite This: *Macromolecules* 2021, 54, 9401−9409 Read Online

ACCESS | Metrics & More | Article Recommendations | Supporting Information

ABSTRACT: Poly(3-hydroxyburtyrate) (P3HB) is the simplest but most important member of the large biodegradable polyhydroxyalkanoate family. However, bacterial P3HB, a pure isotactic crystalline material, is brittle, thus limiting its broad applications. Considering that biodegradable poly(ε-caprolactone) (PCL) and poly(4-hydroxybutyrate) (P4HB) are much more ductile than P3HB, here we utilize metal-catalyzed stereoselective copolymerization of racemic eight-membered dimethyl diolide (*rac*-8DL^{Me}) with ε-caprolactone (ε-CL) and γ-butyrolactone (γ-BL) to toughen P3HB through the formation of isotactic P3HB-based synthetic copolyesters. Notably, catalyst's strong kinetic preference for polymerizing *rac*-8DL^{Me} over ε-CL enables one-pot copolymerization of the 1/1 comonomer mixture to afford diblock copolymer P3HB-*b*-PCL with two crystalline domains (T_{m1} ∼ 55 °C, T_{m2} ∼ 164 °C). Semicrystalline random copolymers, P(3HB-*co*-CL) and P(3HB-*co*-4HB), can also be obtained by simply adjusting the comonomer feed ratio and other polymerization conditions. Mechanical testing showed that P3HB-*b*-PCL is a hard and tough plastic that synergistically combines isotactic P3HB's high modulus with PCL's high ductility.

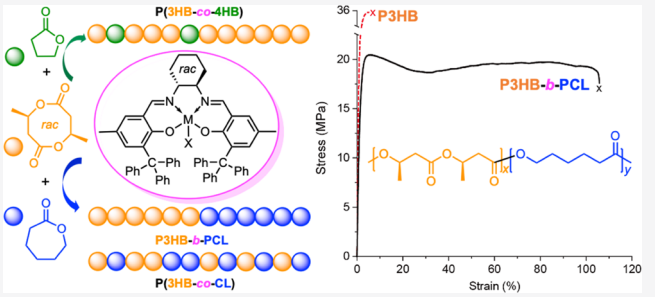

INTRODUCTION

Biodegradable polymers can be returned to enrich the soil by composting them with microorganisms, making them more sustainable promising alternatives to mostly nondegradable commodity polymers such as polyolefins.[1,2] Among them, aliphatic polyesters are the most promising candidates, and in particular, poly(hydroxyalkanoates) (PHAs), which are produced in nature by various microorganisms.[3−14] The simplest and most extensively studied PHA in the large (>150 structures) PHA family is bacterial poly[(*R*)-3-hydroxybutyrate], P[(*R*)-3HB], which is a pure isotactic crystalline thermoplastic material.[3−14] The classic chemical synthesis route to crystalline P3HB is the stereoselective ring-opening polymerization (ROP) of *rac*-β-butyrolactone (*rac*-β-BL), affording syndiotactic P3HB with modest[15−17] to high[18−20] syndiotacticity, or isotactic P3HB with P_m (defined as the probability of *meso* linkages between monomer units) of less than 0.85.[17,21−26] The most recently developed stereoselective ROP of racemic eight-membered cyclic dimethyl diolide (*rac*-8DL^{Me}) by yttrium and lanthanum complexes supported by racemic C_2-symmetric salen ligands (**1** and **2**; Scheme 1) produces rapidly P3HB with essentially quantitative isotacticity (P_m > 0.99, [*mm*] > 99%), high melting-transition temperature (T_m = 171 °C), high number-average molecular weight (M_n = 1.90 × 10^5 g/mol), and low dispersity ($Đ$ = 1.03).[27,28] This highly stereoselective and controlled synthesis has been successfully extended to synthesize other stereoregular PHAs.[28−30] However, although isotactic P3HB exhibits desirable thermal properties (high crystallinity and T_m) and barrier properties (low gas permeability for packaging applications), it has poor mechanical properties due to its brittleness (∼3% elongation at break) and a susceptibility to thermal degradation slightly above its T_m, thus limiting its many potential applications.[31,32]

Copolymerization provides an effective strategy for tailoring the properties of the resulting materials by adjusting the copolymer composition.[33,34] For example, copolymerization of L-lactide and ε-decalactone was used to toughen the brittle polylactide via the incorporation of the flexible polylactone.[35] Copolymerizations of *rac*-8DL^{Me} with *rac*-8DL^{R} (R = ethyl, *n*-butyl) afforded PHA random copolymers with various levels of *rac*-8DL^{R} incorporation and tunable thermal and mechanical properties.[29] In addition, diastereoselective polymerization enabled the direct copolymerization of diastereomeric mixtures of the same or different 8DL^{R} into a stereosequenced semicrystalline stereoblock or tapered stereoblock microstructures.[28] In this work, we aimed to toughen isotactic P3HB through stereoselective copolymerization of *rac*-8DL^{Me}

Received: June 3, 2021
Revised: September 12, 2021
Published: October 7, 2021

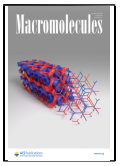

https://doi.org/10.1021/acs.macromol.1c01199
Macromolecules 2021, 54, 9401−9409

Scheme 1. Copolymerization of *rac*-8DL^{Me} with ε-CL or γ-BL by Metal-Based Precatalysts 1 (M = Y) and 2 (M = La)[a]

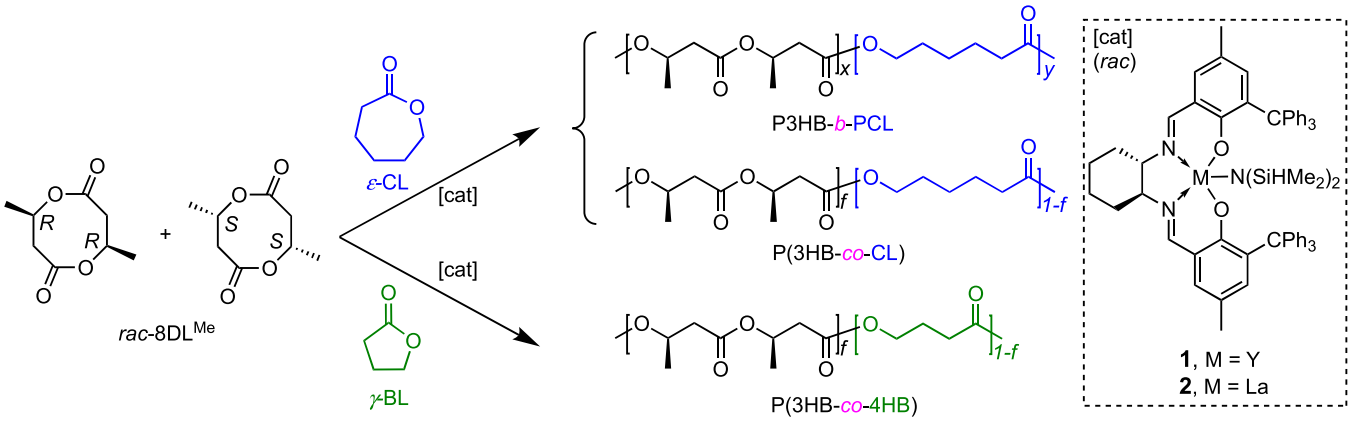

[a]Both precatalysts were employed as racemates.

Table 1. Results of Copolymerization of *rac*-8DL^{Me} with ε-CL[a]

					conv. (%)[b]		[c]	[c]
run	cat	*rac*-8DL^{Me}/ε-CL	[*rac*-8DL^{Me}+ε-CL]/[Cat]	time (min)	*rac*-8DL^{Me}	ε-CL	M_n (kg/mol)	$Đ$ (M_w/M_n)
1	**1**	1/1	200/1	1	98	3.4	11.5	1.04
2	**1**	1/1	200/1	20	100	94	17.4	1.16
3	**1**	1/1	400/1	45	100	93	29.9	1.17
4	**2**	1/1	800/1	1	100	12	58.7	1.03
5	**2**	1/1	800/1	8	100	85	67.0	1.25
6	**2**	1/1	800/1	60	100	95	70.6	1.33
7	**2**	1/2	800/1	1	91	0	n.d.	n.d.

[a]Conditions: *rac*-8DL^{Me} + ε-CL = 1.0 mmol, $V_{solvent}$ = 1.0 mL, CH_2Cl_2 as the solvent, BnOH (1 equiv relative to the catalyst) as the initiator, the catalyst and initiator amount varied according to the [*rac*-8DL^{Me} + ε-CL]/[Cat]/[BnOH] ratio, and ambient temperature (~23 °C). n.d. = not determined. [b]Conversions of *rac*-8DL^{Me} and ε-CL measured by ^{1}H NMR spectra of the quenched solution in benzoic acid/chloroform. [c]Weight-average molecular weights (M_w), number-average molecular weights (M_n), and dispersity indices ($Đ = M_w/M_n$) determined by the gel−permeation chromatography (GPC) coupled with an 18-angle light scattering detector at 40 °C in chloroform.

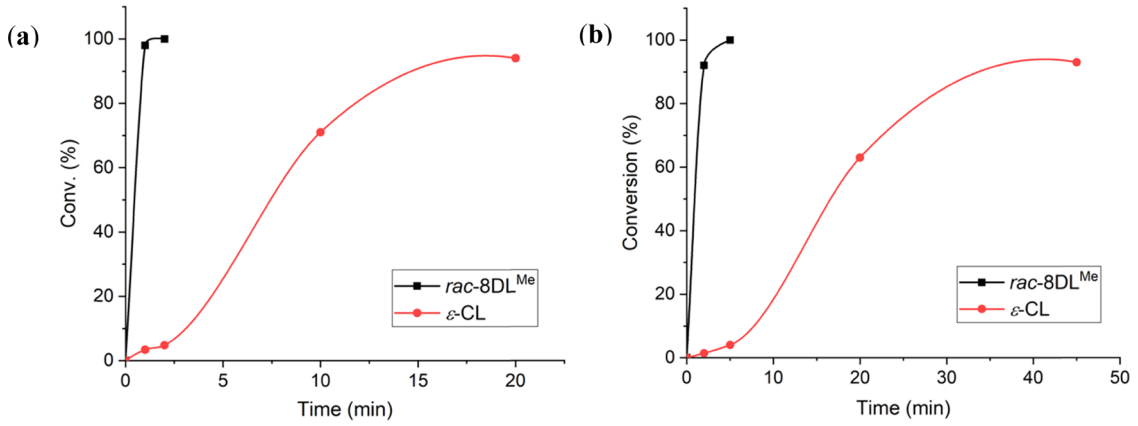

Figure 1. Time-conversion plots for the copolymerization of *rac*-8DL^{Me} and ε-CL (1/1 feed ratio) by catalyst 1 in dichloromethane at ambient temperature: (a) [*rac*-8DL^{Me} + ε-CL]/[1] = 200 (run 2, Table 1) and (b) [*rac*-8DL^{Me} + ε-CL]/[1] = 400 (run 3, Table 1).

with other readily available lactones that can lead to biodegradable and ductile polyesters. In this context, ε-caprolactone (ε-CL) and γ-butyrolactone (γ-BL) become attractive candidates for achieving this objective as their ROP produces biodegradable poly(ε-caprolactone) (PCL)[36−44] and poly(γ-butyrolactone) [PγBL, a structural equivalent of microbial poly(4-hydroxybutyrate), P4HB, also a key member of PHAs)],[45−53] respectively. Both PCL and P4HB have been shown to exhibit better mechanical properties relative to other commonly used aliphatic polyesters,[37,54] and, in particular, they are much more ductile than P3HB. However, their low T_m values (~60 °C) restricted their applications to relatively lower temperatures. Accordingly, we hypothesized that P3HB-based copolymers that incorporate flexible PCL or P4HB units should be synergistically beneficial for enhancing the thermal and mechanical properties of P3HB and PCL or P4HB. This contribution presents an account of the stereoselective copolymerization of *rac*-8DL^{Me} with ε-CL or γ-BL using precatalysts **1** and **2**, which produces isotactic

https://doi.org/10.1021/acs.macromol.1c01199
Macromolecules 2021, 54, 9401−9409

Table 2. Results of Random Copolymerization of *rac*-8DL^{Me} with *ε*-CL[a]

run	cat	[*rac*-8DL^{Me}]/[Cat]	*rac*-8DL^{Me}/*ε*-CL	time (min)	conv. of *rac*-8DL^{Me}[b] (%)	*ε*-CL content[c] (%)	M_n[d] (kg/mol)	$Đ$[d] (M_w/M_n)	T_m[e] (°C)
1	**1**	200/1	1/5	8	89	8.0	17.2	1.05	157
2	**1**	200/1	1/5	12	97	15.5	22.0	1.06	157
3	**1**	200/1	1/10	5	57	11.1	12.4	1.04	150
4	**1**	200/1	1/10	10	72	13.1	15.1	1.05	149
5	**1**	200/1	1/10	25	92	24.9	23.1	1.06	147
6	**1**	400/1	1/10	24 h	64	11.9	24.4	1.05	150
7	**1**	400/1	1/5	30	87	7.1	34.6	1.06	158
8	**1**	600/1	1/5	48 h	61	4.0	32.6	1.05	161
9	**2**	400/1	1/10	20	79	5.5	31.8	1.04	160
10	**2**	400/1	1/10	360	94	9.8	33.8	1.05	161
11	**2**	600/1	1/10	36 h	78	6.3	39.7	1.06	163

[a]Conditions: *rac*-8DL^{Me} = 0.8 mmol, $V_{solvent}$ = 0.8 mL, CH_2Cl_2 as the solvent, BnOH (1 equiv relative to the catalyst) as the initiator, the catalyst and initiator amount varying according to the [*rac*-8DL^{Me}]/[Cat]/[BnOH] ratio, ambient temperature (~23 °C). [b]Conversions of *rac*-8DL^{Me} measured by ^{1}H NMR spectra of the quenched solution in benzoic acid/chloroform. [c]*ε*-CL content measured by ^{1}H NMR of the isolated copolymer. [d]M_w, M_n, and $Đ$ values determined by GPC coupled with an 18-angle light scattering detector at 40 °C in chloroform. [e]Measured by differential scanning calorimetry (DSC) with the cooling and second heating rate of 10 °C/min.

diblock or random copolymers with tunable properties (Scheme 1).

RESULTS AND DISCUSSION

Characteristics of Copolymerization of *rac*-8DL^{Me} with *ε*-CL. As C_2-symmetric chiral complexes **1** and **2** have been shown to catalyze rapid and stereoselective ROP of *rac*-8DL^{Me}, producing P3HB with essentially perfect isotacticity (P_m > 0.99, [*mm*] > 99%) and high molecular weight,[27,28] they were employed in the present study of copolymerization of *rac*-8DL^{Me} with *ε*-CL. With Y-based precatalyst **1**, in combination with 1 equiv of benzyl alcohol (BnOH) that converts *in situ* the silylamide precatalyst to the corresponding alkoxy catalyst,[17−20,55] the copolymerization of *rac*-8DL^{Me} with *ε*-CL in a 1:1 feed ratio and a 0.5 mol % catalyst loading consumed *rac*-8DL^{Me} nearly quantitatively (98%) in just 1 min of the reaction, while the conversion of *ε*-CL only reached 3.4% (run 1, Table 1). The resulting copolymer had a M_n of 11.5 kg/mol and a dispersity ($Đ$) of 1.04. Extending the copolymerization time to 20 min further converted *ε*-CL to achieve a conversion of 94%, thus affording a copolymer with a higher molecular weight and *ε*-CL incorporation (M_n of 17.4 kg/mol, $Đ$ = 1.16, run 2, Table 1). Kinetic profiling of the copolymerization revealed that the catalyst derived from complex **1** exhibits a substantially higher rate of polymerization for *rac*-8DL^{Me} relative to *ε*-CL and thus rapidly consumes *rac*-8DL^{Me} first, followed by slow but gradual consumption of *ε*-CL (Figure 1a and Table S1). The estimated initial k_p, *rac*-8DL^{Me}/k_p, *ε*-CL is 28.8. Therefore, the resulting copolyester is that of a block copolymer, P3HB-*b*-PCL, which was further confirmed by its NMR spectroscopic and thermal property characterizations (*vide infra*).

Similar kinetic profiles (Figure 1b) were also observed for both monomers when the ratio of [*rac*-8DL^{Me} + *ε*-CL]/[**1**] was increased to 400/1 (i.e., 0.25 mol % catalyst loading), which afforded a diblock copolymer P3HB-*b*-PCL with a further enhanced molecular weight of M_n = 29.9 kg/mol and $Đ$ = 1.17 after 45 min, at which point the conversion of *rac*-8DL^{Me} and *ε*-CL was 100% and 93%, respectively (run 3, Table 1). Switching to the La-based catalyst **2**, which is generally more active in polymerizations due to its larger ionic radius as compared to Y-based catalyst **1**, indeed brought about a more rapid polymerization, even with a lower catalyst loading of 0.125 mol % (runs 4−6, Table 1). Similarly, all *rac*-8DL^{Me} was converted to polymer within 1 min, while *ε*-CL polymerization proceeded much more slowly, thus also resulting in block copolymer P3HB-*b*-PCL (M_n = 58.7−70.6 kg/mol, $Đ$ = 1.03−1.33). It is worth noting that the copolymerization of *rac*-8DL^{Me} with *ε*-CL in a 1:2 feed ratio by catalyst **2** converted 91% *rac*-8DL^{Me} in just 1 min (run 7, Table 1), while no conversion of *ε*-CL was observed, indicating that the resulting block copolymer had a little to negligible tapering phase.

The above results demonstrated that the strong kinetic bias of the catalyst toward the polymerization of one of the comonomer pairs [*rac*-8DL^{Me} + *ε*-CL] leads to the formation of *block copolymer* P3HB-*b*-PCL from the copolymerization of the 1:1 monomer mixture. We reasoned that increasing the molar percentage of the slow-reacting monomer *ε*-CL in the feed should alter the copolymer microstructure to favor *random copolymer* formation. In addition, to inhibit the PCL block formation after all *rac*-8DL^{Me} has been depleted in the feed, the copolymerization should be quenched before the full conversion of *rac*-8DL^{Me} is reached. Indeed, applying these two strategies has enabled the successful synthesis of random copolymers, with the representative results summarized in Table 2. Specifically, in the copolymerization with a catalyst **1** loading of 0.5 mol % and a *rac*-8DL^{Me}/*ε*-CL feed ratio of 1/5, the *ε*-CL incorporation in the resulting copolymer increased from 8.0 to 15.5% with the polymerization time increasing from 8 to 12 min, while the *rac*-8DL^{Me} conversion was also increased from 89 to 97% (runs 1 and 2, Table 2). Both the dispersity ($Đ$ = 1.05−1.06) and the melting-transition temperature (T_m = 157 °C) of the resulting copolymer remained the same, presumably due to the higher *ε*-CL incorporation occurring at the late stage of the polymerization with lower *rac*-8DL^{Me} concentration, a scenario that should not affect the T_m of the copolymer noticeably. To further increase the *ε*-CL incorporation, employing a *rac*-8DL^{Me}/*ε*-CL feed ratio of 1/10 afforded copolymers with *ε*-CL incorporations ranging from 11.1 to 24.9% and M_n from 12.4 to 23.1 kg/mol ($Đ$ = 1.04−1.06) at different polymerization times (runs 3−5, Table 2). The copolymers with higher molecular weights of M_n = 24.4−34.6 kg/mol ($Đ$ = 1.05−1.06) were obtained with lower catalyst loadings (runs 6−8, Table 2), but the monomer conversions were limited. Switching to more active La-based **2**,

https://doi.org/10.1021/acs.macromol.1c01199
Macromolecules 2021, 54, 9401−9409

P3HB-*co*-PCL copolymers with higher molecular weights of M_n = 31.8−39.7 kg/mol ($Đ$ = 1.04−1.06) but lower ε-CL incorporations of below 10 mol % (runs 9−11, Table 2) were obtained, which can be attributed to the more pronounced rate enhancement by catalyst **2** for *rac*-8DL^{Me} than that for ε-CL.

Characteristics of Copolymerization of *rac*-8DL^{Me} with γ-BL. The high ductility of P4HB imparts superior mechanical properties as compared to P3HB,[54] and incorporation of 4HB units into P3HB through biological synthesis can enhance the toughness of the resulting copolymer, P3HB-*co*-P4HB.[56,57] Here, we utilize chemical synthesis, through the copolymerization of *rac*-8DL^{Me} with γ-BL, to obtain P(3HB-*co*-4HB). Since γ-BL is "non-polymerizable" under ambient conditions, due to its unfavorable thermodynamics of the polymerization,[50] the copolymerization of *rac*-8DL^{Me} with γ-BL at ambient temperature by Y-based catalyst **1** afforded random copolymer, P(3HB-*co*-4HB), with low γ-BL incorporation of 3.7%, even with a high γ-BL/*rac*-8DL^{Me} feed ratio of 10/1 (run 1, Table 3). It should be noted here that the γ-BL incorporation of 3.7% is the γ-BL incorporation relative to the *rac*-8DL^{Me} monomer, but not the 3HB repeat unit. Increasing the concentration by reducing the amount of the solvent from 0.8 to 0.2 mL increased the γ-BL content to 4.6% in the resulting copolymer (run 2, Table 3), while increasing the temperature did not affect the copolymer composition noticeably (run 3 vs run 1, Table 3). Complex **2** also showed higher activity for this copolymerization than **1**, but it produced the copolymer with an even lower γ-BL incorporation of 2.8% (run 4, Table 3).

Table 3. Results of Copolymerization of *rac*-8DL^{Me} with γ-BL[a]

run	cat	temp. (°C)	time (min)	conv. of *rac*-8DL^{Me}[b] (%)	γ-BL content[c] (%)	M_n[d] (kg/mol)	$Đ$[d] (M_w/M_n)
1	**1**	23	30	93	3.7	16.4	1.05
2[e]	**1**	23	30	92	4.6	18.6	1.05
3	**1**	40	20	77	3.6	14.6	1.04
4	**2**	23	30	100	2.8	18.8	1.05

[a]Conditions: *rac*-8DL^{Me} = 0.8 mmol, $V_{solvent}$ = 0.8 mL, CH_2Cl_2 as the solvent, BnOH as the initiator, [*rac*-8DL^{Me}]/[Cat]/[BnOH] = 200/1/1, and *rac*-8DL^{Me}/γ-BL = 1/10. [b]Conversions of *rac*-8DL^{Me} measured by ^{1}H NMR spectra of the quenched solution in benzoic acid/chloroform. [c]γ-BL content measured by ^{1}H NMR of the isolated copolymer. [d]M_w, M_n, and $Đ$ values determined by GPC coupled with an 18-angle light scattering detector at 40 °C in chloroform. [e]$V_{solvent}$ = 0.2 mL.

Overall, the copolymerization of *rac*-8DL^{Me} with γ-BL under ambient conditions led to random P(3HB-*co*-4HB) copolymers with a narrow range of the γ-BL incorporations (2.8−4.6%) and molecular weights (M_n = 14.6−18.8 kg/mol, $Đ$ = 1.04−1.05). Worth noting here is the fact that the copolymer, thanks to its high isotacticity of the P3HB fraction, is a semicrystalline material and exhibits a high T_m of 159 °C (*vide infra*). This stereochemical control in the copolymerization delivers a superior feature to that of copolymers derived from the copolymerization of *rac*-β-BL with γ-BL, which produced the copolymers with low tacticity (~65% isotactic or syndio-enriched P3HB fraction) and T_m (57−90 °C).[58−60]

Microstructures of P3HB-Based Copolyesters. The microstructures of the copolymers of *rac*-8DL^{Me} with ε-CL and γ-BL were investigated by ^{1}H and ^{13}C NMR methods. Figure 2 depicts ^{1}H NMR spectra of typical random copolymer P(3HB-*co*-CL) and diblock copolymer P3HB-*b*-PCL. The monomer incorporation was calculated by ^{1}H NMR spectra, while ^{13}C NMR spectra provided more detailed information about the microstructure (Figure 3).[61,62] Noting here particularly the ^{13}C NMR spectrum (Figure 3a) of the *random* copolymer P(3HB-*co*-CL), the expanded carbonyl resonances (169.2−173.6 ppm) were resolved into four groups of peaks, arising from different diad sequences of 3HB and CL units (3HB-3HB, 169.2 ppm; 3HB-CL, 170.2 ppm; CL-3HB, 172.7 ppm; and CL-CL, 173.6 ppm). A similar resolution of resonances (64.2−67.7 ppm) for the carbon atom linked to the oxygen atom was also observed. The presence of 3HB-CL and CL-3HB alternating sequences further confirmed the insertion of ε-CL into the resulting copolymer P(3HB-*co*-CL). Importantly, the carbonyl region of the *block* copolymer P3HB-*b*-PCL in the ^{13}C NMR spectrum

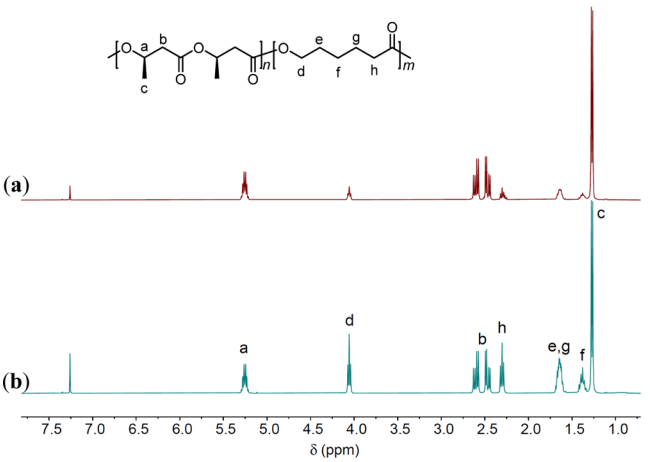

Figure 2. ^{1}H NMR spectra ($CDCl_3$) of (a) random copolymer P(3HB-*co*-CL) with ε-CL incorporation of 24.9% (run 5, Table 2) and (b) block copolymer P3HB-*b*-PCL with PCL content of 48% (run 2, Table 1).

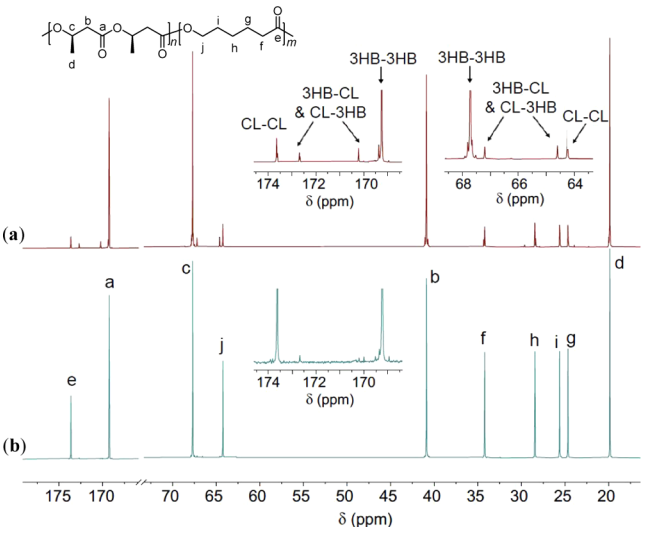

Figure 3. ^{13}C NMR spectra ($CDCl_3$) of (a) random copolymer P(3HB-*co*-CL) with ε-CL incorporation of 24.9% (run 5, Table 2) and (b) block copolymer P3HB-*b*-PCL with PCL content of 48% (run 2, Table 1).

https://doi.org/10.1021/acs.macromol.1c01199
Macromolecules 2021, 54, 9401−9409

(Figure 3b) also showed the peaks for 3HB-CL and CL-3HB alternating sequences but with a much lower intensity, suggesting the copolymer is a block copolymer not a mixture of P3HB and PCL. To further prove that the resultant block copolymer P3HB-*b*-PCL is not a mixture of P3HB and PCL, the solvent extraction method was employed to isolate the possible potential mixture of P3HB and PCL for a physical blend. Since isotactic P3HB shows very poor solubility in tetrahydrofuran (THF) while PCL can dissolve in THF well, THF (80 mL) was utilized to extract the block copolymer (200 mg) prepared with *rac*-8DL^{Me}/ε-CL = 1/1 and [*rac*-8DL^{Me} + ε-CL]/[**1**] = 200 (run 2, Table 1). After stirring in THF for 8 h, 172 mg (86 wt %) of the insoluble fraction was collected, which showed a similar ^{1}H NMR spectrum (Figure S1a) to that of the original polymer (Figure 2a). This result indicated the PCL was linked to P3HB in the form of a block copolymer, making it insoluble in THF. However, the soluble fraction (14 wt %) showed a ^{1}H NMR spectrum (Figure S1b) with a much higher PCL content (97%), ascribed to the small amount of the block copolymer with a very short P3HB block segment produced during the polymerization process. We also examined the block structure of P3HB-*b*-PCL by DOSY NMR analysis, the spectrum of which (Figure S2) exhibited a single diffusion coefficient for the observed signals, thus providing additional evidence for the block copolymer structure as a single component. In contrast, more than one diffusion coefficient was exhibited in the P3HB/PCL physical blend (Figure S3). Overall, these results confirmed that the resulting copolymer prepared with *rac*-8DL^{Me}/ε-CL = 1/1 is indeed a block copolymer.

Likewise, the microstructure of the copolymer P(3HB-*co*-4HB) was characterized by NMR analysis. The ^{1}H NMR spectrum (Figure 4) shows clearly the peaks for each proton of

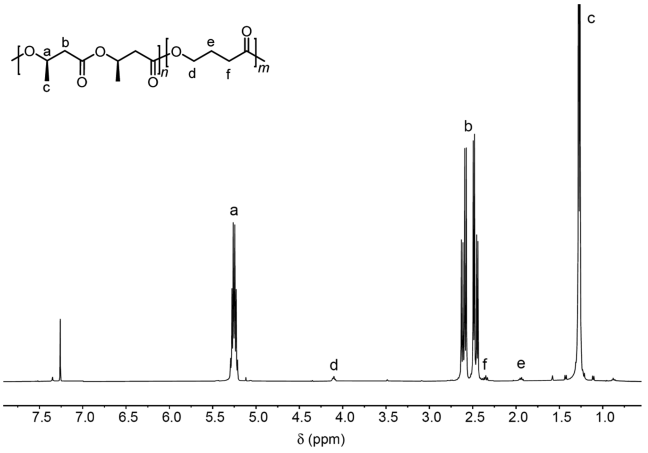

Figure 4. ^{1}H NMR spectrum ($CDCl_3$) of random copolymer P(3HB-*co*-4HB) with γ-BL incorporation of 3.7% (run 1, Table 3).

the copolymer, and in the ^{13}C NMR spectrum (Figure 5), the expanded carbonyl resonances (169.2−173.6 ppm) were resolved into three groups of peaks, arising from different diad sequences of 3HB and 4HB units (3HB-3HB, 169.2 ppm; 3HB-4HB, 170.0 ppm; and 4HB-3HB, 171.9 ppm) without obvious 4HB−4HB continuous sequence,[63] confirming that copolymer P(3HB-*co*-4HB) has a random structure.

Thermal Properties of P3HB-Based Copolyesters. The thermal properties of the block copolymer P3HB-*b*-PCL and random copolymers P(3HB-*co*-CL) and P(3HB-*co*-4HB) were

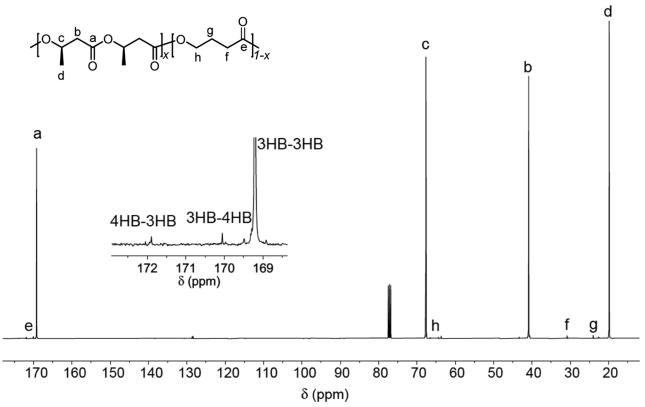

Figure 5. ^{13}C NMR spectrum ($CDCl_3$) of random copolymer P(3HB-*co*-4HB) with γ-BL incorporation of 3.7% (run 1, Table 3).

analyzed by DSC and thermogravimetric analysis (TGA) methods. When the copolymerization of *rac*-8DL^{Me} and ε-CL (1/1) by catalyst **1** was quenched before generating the PCL block (run 1, Table 1), one crystallization temperature (T_c) and one T_m for the isotactic P3HB segment was observed on the first cooling and second heating scans of the DSC curve, respectively (Figure S4). After extending the polymerization time to full conversions of both monomers (run 2, Table 1), the resulting block copolymer (M_n = 17.4 kg/mol, PCL% = 48%, run 2, Table 1) exhibited two T_c's at 7.0 and 48.0 °C and two T_m's at 54.6 and 162 °C (Figure 6a), corresponding to the PCL and P3HB block. Likewise, the higher-molecular-weight block copolymer produced by catalyst **2** (M_n = 70.6 kg/mol, PCL% = 49%, run 6, Table 1) also exhibited two T_c's at 24.5 and 67.8 °C and two T_m's at 54.4 and 166 °C (Figure 6b). Overall, these thermal analysis results collaborate well with the above-described kinetic profiling and spectroscopic signatures, further confirming the formation of the block copolymer P3HB-*b*-PCL through the copolymerization of the one-pot monomer mixture.

For the random copolymers P(3HB-*co*-CL), generally, copolymers with higher ε-CL incorporations exhibited lower T_m's, as expected and shown in Figures 7 and S5−13. In addition, the crystallization rate of the random copolymers with higher ε-CL incorporations became slow. For example, although the T_m (147 °C) of the random copolymer with higher ε-CL incorporation of 24.9% is just 2 °C lower than that with lower ε-CL incorporation of 13.1% (Figure 7b vs S7), the T_c (65.8 °C) for the copolymer with 24.9% ε-CL incorporation was observed only on the second DSC heating scan but not on the first cooling scan (Figure 7b), indicating its lower crystallization rate. In contrast, the random copolymer with 13.1 or 8.0% ε-CL incorporation can be crystallized nearly completely (Figure S7) or completely (Figure 7a) on the first cooling cycle, as evidenced by the appearance of a larger exothermic T_c peak (71.5 °C) on cooling, which was absent on the second heating scan (Figure 7a). The copolymer P(3HB-*co*-4HB) with γ-BL incorporation of 3.7% (M_n = 16.4 kg/mol, run 1, Table 3) showed a T_m of 159 °C (Figure 8), which is somewhat lower than that of isotactic P3HB with a similar molecular weight (161 °C).[27]

TGA and relative derivative thermogravimetry (DTG) curves of the block copolymer P3HB-*b*-PCL prepared by catalyst **2** (M_n = 70.6 kg/mol, PCL% = 49%, run 6, Table 1) displayed two degradation steps (Figure 9a), attributed to the P3HB block degradation at a lower initial degradation

https://doi.org/10.1021/acs.macromol.1c01199
Macromolecules 2021, 54, 9401−9409

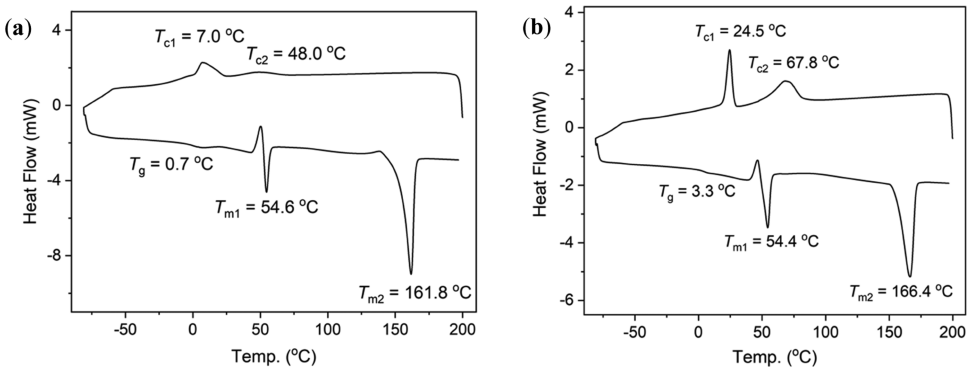

Figure 6. DSC curves of block copolymers P3HB-*b*-PCL: (a) prepared by catalyst **1**, PCL% = 48% (run 2, Table 1) and (b) prepared by catalyst **2**, PCL% = 49% (run 6, Table 1).

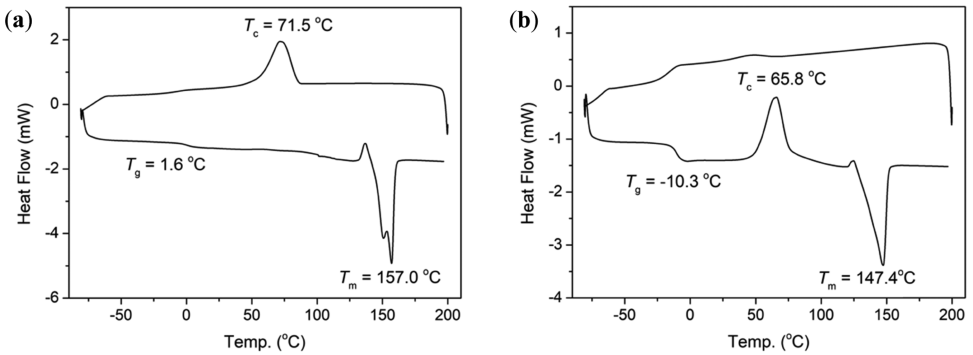

Figure 7. DSC curves of random copolymers P(3HB-*co*-CL) produced by **1** with different ε-CL incorporations: (a) PCL% = 8.0% (run 1, Table 2) and (b) PCL% = 24.9% (run 5, Table 2).

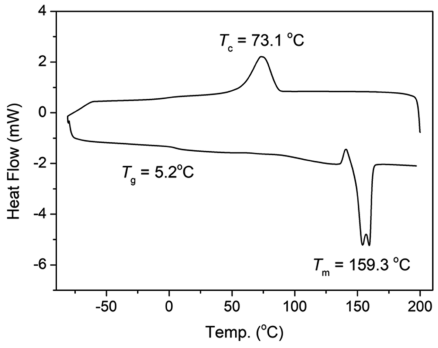

Figure 8. DSC curve of the random copolymer P(3HB-*co*-4HB) produced by complex **1** with γ-BL incorporation of 3.7% (run 1, Table 3).

temperature (T_d, defined by the temperature of 5% weight loss) of 239 °C and PCL block degradation at a higher temperature of 302 °C, with their corresponding T_{max} (maximum rate of decomposition temperature) values of 259 and 327 °C. In contrast, random copolymer P(3HB-*co*-CL) (M_n = 17.2 kg/mol, ε-CL incorporation of 8.0 mol %; run 1, Table 2) showed only one degradation step with a T_d of 222 °C and a T_{max} of 265 °C (Figure 9b), further confirming its random structure. However, if the polymerization was prolonged to 12 min with the *rac*-8DL^{Me} conversion of 97% at which point the ε-CL incorporation reached 15.5 mol %, the resulting copolymer exhibited a small, second degradation step at higher temperature (T_{max2} = 306 °C, Figure S16). It was attributed to the fact that the higher ε-CL incorporation occurred during a prolonged time period with a much lower *rac*-8DL^{Me} concentration, thus resulting in the nonuniform copolymer chain with a much higher ε-CL incorporation at one end of the copolymer chain, which showed the higher degradation temperature. Consistent with its random copolymer structure, P(3HB-*co*-4HB) with a low level of γ-BL incorporation of 3.7% (run 1, Table 3) exhibited only one degradation step with a T_d of 222 °C and a T_{max} of 261 °C (Figure S19).

Mechanical Properties of P3HB-Based Copolyesters. Tensile testing of a dog-bone-shaped block copolymer P3HB-*b*-PCL (M_n = 70.6 kg/mol, 48.7% PCL, prepared by catalyst **2**, run 6, Table 1) specimens, prepared by compression molding, yielded a stress/strain curve (Figure 10a) with an ultimate tensile strength (σ_B) of 20.5 MPa, Young's modulus (E) of 1.45 GPa, and elongation at break (ε_B) of 106%. Thus, it showed a comparably high Young's modulus but a much larger elongation at break as compared to those of isotactic P3HB (E ~ 3 GPa, ε_B ~ 3%)[12] and a higher Young's modulus than that of PCL (M_n = 204 kg/mol, also prepared by catalyst **2**), with E = 587 ± 19 MPa, ε_B = 698 ± 30%, and σ_B = 39.6 ± 1.4 MPa (Figure 10b). It is worth noting that the block copolymer P3HB-*b*-PCL also exhibited a higher Young's modulus, elongation at break, and tensile strength than P3HB/PCL blends (P3HB/PCL wt. ratio of 77/23: E = 730 MPa, ε_B = 9%, and σ_B = 21 MPa; P3HB/PCL wt. ratio of 49/51: E = 110 MPa, ε_B = 18%, and σ_B = 4 MPa).[64] These results suggested that the block copolymer P3HB-*b*-PCL can combine the advantages of a high Young's modulus of isotactic P3HB and a large elongation at break of PCL, making it a hard and tough plastic. For comparison with the block copolymer P3HB-*b*-PCL, the random copolymer P(3HB-*co*-CL) (prepared by

https://doi.org/10.1021/acs.macromol.1c01199
Macromolecules 2021, 54, 9401−9409

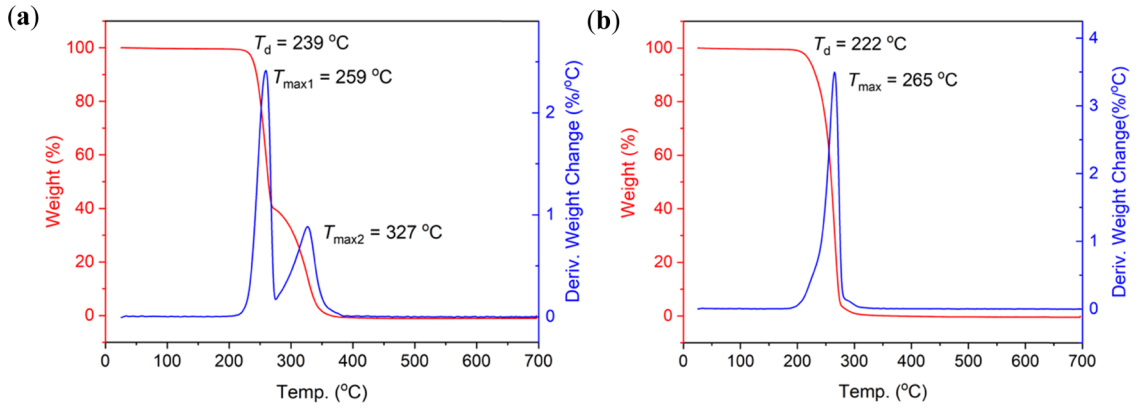

Figure 9. TGA (red) and DTG (blue) curves of (a) block copolymer P3HB-*b*-PCL (PCL% = 49 mol %; run 6, Table 1) and (b) the random copolymer P(3HB-*co*-CL) with ε-CL incorporation of 8.0 mol % (run 1, Table 2).

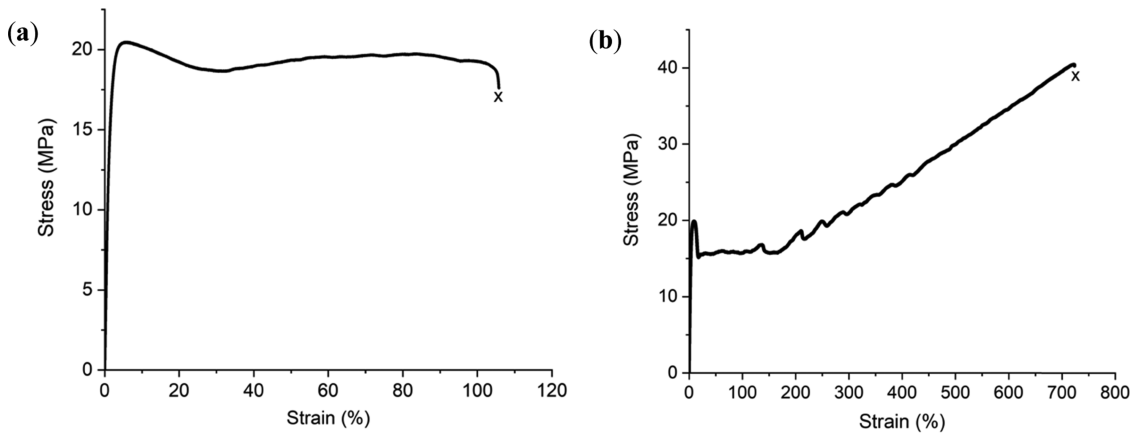

Figure 10. Stress−strain curves (10 mm/min, ambient temperature) of (a) block copolymer P3HB-*b*-PCL (M_n = 70.6 kg/mol) prepared by catalyst **2 and** (b) PCL (M_n = 204 kg/mol) also prepared by catalyst **2**. Break point indicated by "x".

catalyst **1**, run 5, Table 2) was also tested for its mechanical performance (Figure S27), giving a comparable ultimate tensile strength of 22.3 MPa, but a lower Young's modulus of 740 MPa and much lower elongation at break of only 7.6% due to its lower molecular weight (M_n = 23.1 kg/mol) and ε-CL content (~25%).

CONCLUSIONS

Stereoselective copolymerization was employed to overcome the high brittleness of isotactic P3HB while taking advantage of its high crystallinity and crystallization rate by incorporating flexible ε-CL and γ-BL units into the resulting copolyester. The copolymerization of *rac*-8DL^{Me} with ε-CL can produce either block copolymers P3HB-*b*-PCL or random copolymers P(3HB-*co*-CL) in a one-pot fashion, depending on the polymerization conditions, particularly the *rac*-8DL^{Me}/ε-CL molar ratio. When copolymerizations were conducted with the *rac*-8DL^{Me}/ε-CL molar ratio of 1/1, block copolymers P3HB-*b*-PCL with M_n up to 77.8 kg/mol can be obtained. On the other hand, random copolymer P(3HB-*co*-CL) was produced with the *rac*-8DL^{Me}/ε-CL molar ratio of 1/5~1/10 when the copolymerization was quenched before the full conversion of *rac*-8DL^{Me}. The ε-CL incorporation into the random copolymer can be tuned from 4.0 to 24.9%, giving random copolymers with M_n = 12.4−39.7 kg/mol and $Đ$ = 1.04−1.06. Likewise, semicrystalline random copolymers P(3HB-*co*-4HB) with low γ-BL incorporations of 2.8−4.6% but a high T_m of 159 °C can be obtained by the copolymerization of *rac*-8DL^{Me} with γ-BL under ambient conditions.

Collaborative evidence obtained from the kinetic profiling of the copolymerization, ^{1}H and ^{13}C NMR characterizations of copolymer microstructures, and thermal transition and degradation analysis demonstrated the block copolymer formation from the copolymerization of the one-pot 1/1 comonomer mixture. On thermal transitions, the block copolymers P3HB-*b*-PCL are characterized by displaying two crystallization temperatures upon crystallization and thus exhibit two crystalline domains with the first T_m around 55 °C for the PCL block and the second T_m around 162−166 °C for the isotactic P3HB block. On thermal degradation, the block copolymers show two degradation steps, corresponding to the P3HB block degradation at a lower initial degradation temperature (T_{max} ~ 260 °C) and the PCL block degradation at a higher temperature (T_{max} ~ 330 °C). In contrast, random copolymer P(3HB-*co*-CL) showed only one T_c and one T_m, the values of which are dependent on the ε-CL incorporation in the copolymer, and one degradation step with a T_d of 222 °C and a T_{max} of 265 °C. Notably, the block copolymer P3HB-*b*-PCL is a hard and tough plastic with an ultimate tensile strength of 20.5 MPa, Young's modulus of 1.45 GPa, and elongation at break of 106%. Therefore, the block copolymer combines the advantages of a high modulus of isotactic P3HB and a large elongation at break of PCL.

https://doi.org/10.1021/acs.macromol.1c01199
Macromolecules 2021, 54, 9401−9409

■ ASSOCIATED CONTENT

Supporting Information

The Supporting Information is available free of charge at https://pubs.acs.org/doi/10.1021/acs.macromol.1c01199.

Conversion data of *rac*-DL^{Me} and ϵ-CL copolymerizations by catalysts 1-2 and BnOH initiator; ^{1}H NMR spectra; DOSY NMR spectrum; DSC curves of the block copolymer, random copolymer, TGA (red) and DTG (blue) curves of the block copolymer, and random copolymer; GPC trace of the block copolymer and random copolymer; and stress−strain curve (10 mm/min, ambient temperature) of random copolymer (PDF)

■ AUTHOR INFORMATION

Corresponding Authors

Xiaoyan Tang − *Department of Chemistry, Colorado State University, Fort Collins, Colorado 80523-1872, United States; Beijing National Laboratory for Molecular Sciences, Key Laboratory of Polymer Chemistry and Physics of Ministry of Education, Center for Soft Matter Science and Engineering, College of Chemistry and Molecular Engineering, Peking University, Beijing 100871, China;* orcid.org/0000-0002-0050-6699; Email: xiaoyan.tang@pku.edu.cn

Eugene Y.-X. Chen − *Department of Chemistry, Colorado State University, Fort Collins, Colorado 80523-1872, United States;* orcid.org/0000-0001-7512-3484; Email: eugene.chen@colostate.edu

Authors

Changxia Shi − *Department of Chemistry, Colorado State University, Fort Collins, Colorado 80523-1872, United States*

Zhen Zhang − *Department of Chemistry, Colorado State University, Fort Collins, Colorado 80523-1872, United States*

Complete contact information is available at: https://pubs.acs.org/10.1021/acs.macromol.1c01199

Notes

The authors declare no competing financial interest.

■ ACKNOWLEDGMENTS

The work was supported by the US National Science Foundation (NSF-1955482) to E.Y.-X.C. and Peking University Ge Li and Ning Zhao Life Science Research Fund for Young Scientists to X.T.

■ REFERENCES

(1) Chen, G.-Q.; Patel, M. K. Plastics Derived from Biological Sources: Present and Future: A Technical and Environmental Review. *Chem. Rev.* **2012**, *112*, 2082−2099.

(2) Tullo, A. H. PHA: a biopolymer whose time has finally come. *Chem. Eng. News* **2019**, *97*, 20−21.

(3) Anjum, A.; Zuber, M.; Zia, K. M.; Noreen, A.; Anjum, M. N.; Tabasum, S. Microbial production of polyhydroxyalkanoates (PHAs) and its copolymers: A review of recent advancements. *Int. J. Biol. Macromol.* **2016**, *89*, 161−174.

(4) Li, Z.; Yang, J.; Loh, X. J. Polyhydroxyalkanoates: opening doors for a sustainable future. *NPG Asia Mater.* **2016**, *8*, No. e265.

(5) Muhammadi; Shabina; Afzal, M.; Hameed, S. Bacterial polyhydroxyalkanoates-eco-friendly next generation plastic: Production, biocompatibility, biodegradation, physical properties and applications. *Green Chem. Lett. Rev.* **2015**, *8*, 56−77.

(6) Laycock, B.; Halley, P.; Pratt, S.; Werker, A.; Lant, P. The chemomechanical properties of microbial polyhydroxyalkanoates. *Prog. Polym. Sci.* **2013**, *38*, 536−583.

(7) Somleva, M. N.; Peoples, O. P.; Snell, K. D. PHA Bioplastics, Biochemicals, and Energy from Crops. *Plant Biotechnol. J.* **2013**, *11*, 233−252.

(8) Taguchi, S.; Iwata, T.; Abe, H.; Doi, Y. 9.09 - Poly(hydroxyalkanoate)s. In *Polymer Science: A Comprehensive Reference*; Matyjaszewski, K.; Möller, M., Eds.; Elsevier: Amsterdam, 2012; pp 157−182.

(9) Chen, G.-Q. Plastics Completely Synthesized by Bacteria: Polyhydroxyalkanoates In *Plastics from Bacteria: Natural Functions and Applications*; Chen, G.-Q., Ed.; Springer-Verlag: Berlin, 2010; Vol. *14*, pp 17−37.

(10) Chen, G.-Q. A microbial polyhydroxyalkanoates (PHA) based bio- and materials industry. *Chem. Soc. Rev.* **2009**, *38*, 2434−2446.

(11) Lenz, R. W.; Marchessault, R. H. Bacterial Polyesters: Biosynthesis, Biodegradable Plastics and Biotechnology. *Biomacromolecules* **2005**, *6*, 1−8.

(12) Sudesh, K.; Abe, H.; Doi, Y. Synthesis, structure and properties of polyhydroxyalkanoates: biological polyesters. *Prog. Polym. Sci.* **2000**, *25*, 1503−1555.

(13) Poirier, Y.; Nawrath, C.; Somerville, C. Production of Polyhydroxyalkanoates, a Family of Biodegradable Plastics and Elastomers, in Bacteria and Plants. *Nat. Biotechnol.* **1995**, *13*, 142.

(14) Müller, H.-M.; Seebach, D. Poly(hydroxyalkanoates): A Fifth Class of Physiologically Important Organic Biopolymers? *Angew. Chem., Int. Ed.* **1993**, *32*, 477−502.

(15) Kemnitzer, J. E.; McCarthy, S. P.; Gross, R. A. Syndiospecific ring-opening polymerization of.beta.-butyrolactone to form predominantly syndiotactic poly(.beta.-hydroxybutyrate) using tin(IV) catalysts. *Macromolecules* **1993**, *26*, 6143−6150.

(16) Kricheldorf, H. R.; Eggerstedt, S. Polylactones. 41. Polymerizations of β-d,l-Butyrolactone with Dialkyltinoxides as Initiators. *Macromolecules* **1997**, *30*, 5693−5697.

(17) Zhuo, Z.; Zhang, C.; Luo, Y.; Wang, Y.; Yao, Y.; Yuan, D.; Cui, D. Stereo-selectivity switchable ROP of rac-β-butyrolactone initiated by salan-ligated rare-earth metal amide complexes: the key role of the substituents on ligand frameworks. *Chem. Commun.* **2018**, *54*, 11998−12001.

(18) Amgoune, A.; Thomas, C. M.; Ilinca, S.; Roisnel, T.; Carpentier, J.-F. Highly Active, Productive, and Syndiospecific Yttrium Initiators for the Polymerization of Racemic β-Butyrolactone. *Angew. Chem., Int. Ed.* **2006**, *45*, 2782−2784.

(19) Ajellal, N.; Bouyahyi, M.; Amgoune, A.; Thomas, C. M.; Bondon, A.; Pillin, I.; Grohens, Y.; Carpentier, J.-F. Syndiotactic-Enriched Poly(3-hydroxybutyrate)s via Stereoselective Ring-Opening Polymerization of Racemic β-Butyrolactone with Discrete Yttrium Catalysts. *Macromolecules* **2009**, *42*, 987−993.

(20) Bouyahyi, M.; Ajellal, N.; Kirillov, E.; Thomas, C. M.; Carpentier, J.-F. Exploring Electronic versus Steric Effects in Stereoselective Ring-Opening Polymerization of Lactide and β-Butyrolactone with Amino-alkoxy-bis(phenolate)−Yttrium Complexes. *Chem. - Eur. J.* **2011**, *17*, 1872−1883.

(21) Bloembergen, S.; Holden, D. A.; Bluhm, T. L.; Hamer, G. K.; Marchessault, R. H. Stereoregularity in synthetic β-hydroxybutyrate and β-hydroxyvalerate homopolyesters. *Macromolecules* **1989**, *22*, 1656−1663.

(22) Le Borgne, A.; Spassky, N. Stereoelective polymerization of β-butyrolactone. *Polymer* **1989**, *30*, 2312−2319.

(23) Jaimes, C.; Arcana, M.; Brethon, A.; Mathieu, A.; Schue, F.; Desimone, J. M. Structure and morphology of poly([R,S]-β-butyrolactone) synthesized from aluminoxane catalyst. *Eur. Polym. J.* **1998**, *34*, 175−185.

(24) Zintl, M.; Molnar, F.; Urban, T.; Bernhart, V.; Preishuber-Pflügl, P.; Rieger, B. Variably isotactic poly(hydroxybutyrate) from racemic β-butyrolactone: Microstructure control by achiral chromium(III) salophen complexes. *Angew. Chem., Int. Ed.* **2008**, *47*, 3458−3460.

(25) Ajellal, N.; Durieux, G.; Delevoye, L.; Tricot, G.; Dujardin, C.; Thomas, C. M.; Gauvin, R. M. Polymerization of racemic β-butyrolactone using supported catalysts: a simple access to isotactic polymers. *Chem. Commun.* **2010**, *46*, 1032−1034.
(26) Yang, L.; Zhang, Y.-Y.; Yang, G.-W.; Xie, R.; Wu, G.-P. Controlled ring-opening polymerization of β-butyrolactone via bifunctional organoboron catalysts. *Macromolecules* **2021**, *54*, 5509−5517.
(27) Tang, X.; Chen, E. Y.-X. Chemical synthesis of perfectly isotactic and high melting bacterial poly(3-hydroxybutyrate) from bio-sourced racemic cyclic diolide. *Nat. Commun.* **2018**, *9*, No. 2345.
(28) Tang, X.; Westlie, A. H.; Watson, E. M.; Chen, E. Y.-X. Stereosequenced crystalline polyhydroxyalkanoates from diastereomeric monomer mixtures. *Science* **2019**, *366*, 754−758.
(29) Tang, X.; Westlie, A. H.; Caporaso, L.; Cavallo, L.; Falivene, L.; Chen, E. Y.-X. Biodegradable Polyhydroxyalkanoates by Stereoselective Copolymerization of Racemic Diolides: Stereocontrol and Polyolefin-Like Properties. *Angew. Chem., Int. Ed.* **2020**, *59*, 7881−7890.
(30) Westlie, A. H.; Chen, E. Y.-X. Catalyzed Chemical Synthesis of Unnatural Aromatic Polyhydroxyalkanoate and Aromatic−Aliphatic PHAs with Record-High Glass-Transition and Decomposition Temperatures. *Macromolecules* **2020**, *53*, 9906−9915.
(31) Sangroniz, A.; Zhu, J.-B.; Tang, X.; Etxeberria, A.; Chen, E. Y.-X.; Sardon, H. Packaging materials with desired mechanical and barrier properties and full chemical recyclability. *Nat. Commun.* **2019**, *10*, No. 3559.
(32) Moore, T.; Adhikari, R.; Gunatillake, P. Chemosynthesis of bioresorbable poly(γ-butyrolactone) by ring-opening polymerisation: a review. *Biomaterials* **2005**, *26*, 3771−3782.
(33) Nakamura, A.; Ito, S.; Nozaki, K. Coordination−insertion copolymerization of fundamental polar monomers. *Chem. Rev.* **2009**, *109*, 5215−5244.
(34) Song, Q.; Pascouau, C.; Zhao, J.; Zhang, G.; Peruch, F.; Carlotti, S. Ring-opening polymerization of γ-lactones and copolymerization with other cyclic monomers. *Prog. Polym. Sci.* **2020**, *110*, No. 101309.
(35) Olsén, P.; Borke, T.; Odelius, K.; Albertsson, A.-C. ε-Decalactone: A thermoresilient and toughening comonomer to poly(l-lactide). *Biomacromolecules* **2013**, *14*, 2883−2890.
(36) Agarwal, S.; Mast, C.; Dehnicke, K.; Greiner, A. Rare earth metal initiated ring-opening polymerization of lactones. *Macromol. Rapid Commun.* **2000**, *21*, 195−212.
(37) Labet, M.; Thielemans, W. Synthesis of polycaprolactone: a review. *Chem. Soc. Rev.* **2009**, *38*, 3484−3504.
(38) Sutar, A. K.; Maharana, T.; Dutta, S.; Chen, C.-T.; Lin, C.-C. Ring-opening polymerization by lithium catalysts: an overview. *Chem. Soc. Rev.* **2010**, *39*, 1724−1746.
(39) Dagorne, S.; Normand, M.; Kirillov, E.; Carpentier, J.-F. Gallium and indium complexes for ring-opening polymerization of cyclic ethers, esters and carbonates. *Coord. Chem. Rev.* **2013**, *257*, 1869−1886.
(40) Carpentier, J.-F. Rare-Earth Complexes Supported by Tripodal Tetradentate Bis(phenolate) Ligands: A Privileged Class of Catalysts for Ring-Opening Polymerization of Cyclic Esters. *Organometallics* **2015**, *34*, 4175−4189.
(41) Guillaume, S. M.; Kirillov, E.; Sarazin, Y.; Carpentier, J.-F. Beyond stereoselectivity, switchable catalysis: Some of the last frontier challenges in ring-opening polymerization of cyclic esters. *Chem. - Eur. J.* **2015**, *21*, 7988−8003.
(42) Piotrowska, U.; Sobczak, M. Enzymatic polymerization of cyclic monomers in ionic liquids as a prospective synthesis method for polyesters used in drug delivery systems. *Molecules* **2015**, *20*, 1−23.
(43) Fuoco, T.; Pappalardo, D. Aluminum alkyl complexes bearing salicylaldiminato ligands: Versatile initiators in the ring-opening polymerization of cyclic esters. *Catalysts* **2017**, *7*, 64.
(44) Li, X.; Chen, C.; Wu, J. Lewis pair catalysts in the polymerization of lactide and related cyclic esters. *Molecules* **2018**, *23*, 189.
(45) Korte, F.; Glet, W. Hochdruckreaktionen. II. Die polymerisation von γ-butyrolacton und δ-valerolactam bei hohen drücken. *J. Polym. Sci., Part B: Polym. Lett.* **1966**, *4*, 685−689.
(46) Nobes, G. A. R.; Kazlauskas, R. J.; Marchessault, R. H. Lipase-catalyzed ring-opening polymerization of lactones: A novel route to poly(hydroxyalkanoate)s. *Macromolecules* **1996**, *29*, 4829−4833.
(47) Oishi, A.; Taguchi, Y.; Fujita, K.; Ikeda, Y.; Masuda, T. Production of poly-γ-butyrolactone. JP Patent JP20002817672000.
(48) Oishi, A.; Taguchi, Y.; Fujita, K. Production method of poly(γ-butyrolactone) using metal complex catalyst. JP Patent JP20032529682003.
(49) Yamashita, K.; Yamamoto, K.; Kadokawa, J.-i. Acid-catalyzed ring-opening polymerization of γ-butyrolactone under high-pressure conditions. *Chem. Lett.* **2014**, *43*, 213−215.
(50) Hong, M.; Chen, E. Y.-X. Completely recyclable biopolymers with linear and cyclic topologies via ring-opening polymerization of γ-butyrolactone. *Nat. Chem.* **2016**, *8*, 42−49.
(51) Hong, M.; Chen, E. Y.-X. Towards truly sustainable polymers: A metal-free recyclable polyester from biorenewable non-strained γ-butyrolactone. *Angew. Chem., Int. Ed.* **2016**, *55*, 4188−4193.
(52) Zhao, N.; Ren, C.; Li, H.; Li, Y.; Liu, S.; Li, Z. Selective ring-opening polymerization of non-strained γ-butyrolactone catalyzed by a cyclic trimeric phosphazene base. *Angew. Chem., Int. Ed.* **2017**, *56*, 12987−12990.
(53) Tang, J.; Chen, E. Y.-X. Effects of Chain Ends on Thermal and Mechanical Properties and Recyclability of Poly(γ-butyrolactone). *J. Polym. Sci., Part A: Polym. Chem.* **2018**, *56*, 2271−2279.
(54) Martin, D. P.; Williams, S. F. Medical applications of poly-4-hydroxybutyrate: a strong flexible absorbable biomaterial. *Biochem. Eng. J.* **2003**, *16*, 97−105.
(55) Amgoune, A.; Thomas, C. M.; Roisnel, T.; Carpentier, J.-F. Ring-opening polymerization of lactide with group 3 metal complexes supported by dianionic alkoxy-amino-bisphenolate ligands: Combining high activity, productivity, and selectivity. *Chem. - Eur. J.* **2006**, *12*, 169−179.
(56) Doi, Y.; Segawa, A.; Kunioka, M. Biosynthesis and characterization of poly(3-hydroxybutyrate-co-4-hydroxybutyrate) in Alcaligenes eutrophus. *Int. J. Biol. Macromol.* **1990**, *12*, 106−111.
(57) Saito, Y.; Doi, Y. Microbial synthesis and properties of poly(3-hydroxybutyrate-co-4-hydroxybutyrate) in Comamonas acidovorans. *Int. J. Biol. Macromol.* **1994**, *16*, 99−104.
(58) Lee, C. W.; Urakawa, R.; Kimura, Y. Copolymerization of γ-butyrolactone and β-butyrolactone. *Macromol. Chem. Phys.* **1997**, *198*, 1109−1120.
(59) Wu, B.; Lenz, R. W.; Scherer, T. M. Preparation, properties and biodegradation of stereoregular copolymers of (R,S)-3-butyrolactone and 4-butyrolactone. *Macromol. Chem. Phys.* **1998**, *199*, 2079−2085.
(60) Wei, Z.; Liu, L.; Qi, M. Synthesis and characterization of homo- and co-polymers of (R,S)-β-butyrolactone and γ-butyrolactone or β-valerolactone initiated with cyclic tin alkoxide. *React. Funct. Polym.* **2006**, *66*, 1411−1419.
(61) Nakayama, A.; Kawasaki, N.; Aiba, S.; Maeda, Y.; Arvanitoyannis, I.; Yamamoto, N. Synthesis and biodegradability of novel copolyesters containg γ-butyrolactone units. *Polymer* **1998**, *39*, 1213−1222.
(62) Hong, M.; Tang, X.; Newell, B. S.; Chen, E. Y.-X. "Nonstrained" γ-Butyrolactone-Based Copolyesters: Copolymerization Characteristics and Composition-Dependent (Thermal, Eutectic, Cocrystallization, and Degradation) Properties. *Macromolecules* **2017**, *50*, 8469−8479.
(63) Doi, Y.; Kunioka, M.; Nakamura, Y.; Soga, K. Nuclear magnetic resonance studies on unusual bacterial copolyesters of 3-hydroxybutyrate and 4-hydroxybutyrate. *Macromolecules* **1988**, *21*, 2722−2727.
(64) Kumagai, Y.; Doi, Y. Enzymatic degradation and morphologies of binary blends of microbial poly(3-hydroxy butyrate) with poly(ε-caprolactone), poly(1,4-butylene adipate and poly(vinyl acetate). *Polym. Degrad. Stab.* **1992**, *36*, 241−248.

https://doi.org/10.1021/acs.macromol.1c01199
Macromolecules 2021, 54, 9401−9409